Journal of Aerosol Science 113 (2017) 95–107

Contents lists available at ScienceDirect

Journal of Aerosol Science

journal homepage: www.elsevier.com/locate/jaerosci

Impact of drought and normal monsoon scenarios on aerosol induced radiative forcing and atmospheric heating in Varanasi over middle Indo-Gangetic Plain

Manish Kumar[a], M.P. Raju[b], R.S. Singh[c,d], Tirthankar Banerjee[a,d,*]

[a] Institute of Environment and Sustainable Development, Banaras Hindu University, Varanasi, India
[b] National Centre for Medium Range Weather Forecasting, Noida, India
[c] Department of Chemical Engineering and Technology, Indian Institute of Technology (BHU), Varanasi, India
[d] DST-Mahamana Centre of Excellence in Climate Change Research, Banaras Hindu University, Varanasi, India

ARTICLE INFO

Keywords:
Black carbon
Indo-Gangetic Plain
Drought
Monsoon
Radiative forcing

ABSTRACT

Observations on aerosols with specific emphasis to black carbon (BC) are reported for an urban site over middle Indo-Gangetic Plain (IGP), South Asia. Emphases are made to evaluate variation in BC concentrations during typical monsoon season (June-September, JJAS) from 2009 to 2011, and to recognize its impact on aerosol radiative forcing (ARF) and atmospheric heating. Almost entire Indian sub-continent experienced a drought year in 2009 before achieving a normal monsoon in 2010 and 2011. The ground monitoring station in Varanasi over middle-IGP experienced minimum monsoonal rain during 2009 drought year (total monsoon rain: 437.3 mm), which gradually increased during 2010 (deficit monsoon, 613.4 mm), before achieving a normal monsoon in year 2011 (1207.0 mm). The BC mass loading during drought year was relatively high (mean ± SD: 7.0 ± 3.3; range: 5.3–8.8 $\mu g\ m^{-3}$) compared to 2010 (4.9 ± 2.1, 3.7–5.8 $\mu g\ m^{-3}$) and 2011 (4.6 ± 2.1, 3.2–5.2 $\mu g\ m^{-3}$). The increase in BC aerosols especially during drought year was associated to lower wind speed and reduced rate of wet removal, which potentially enhanced BC loading in comparison to years with normal monsoon. Columnar aerosol loading in terms of aerosol optical depth (AOD) was retrieved from space-borne MODerate resolution Imaging Spectroradiometer (MODIS) sensor on-board Terra satellite. It has revealed high AOD over Varanasi during drought (2009: 1.03 ± 0.15) and deficit monsoon (2010: 1.07 ± 0.53) before being reduced during 2011 (0.89 ± 0.20). Conclusively, a radiative transfer model was run to estimate the ARF for composite aerosols for both surface (SUF), atmosphere (ATM) and top of the atmosphere (TOA). The 2009 drought year was found to have reasonably higher ATM and SUF forcing (ATM: 105; SUF: − 122 $W\ m^{-2}$) in comparison to deficit (ATM: 61; SUF: − 88 $W\ m^{-2}$) and normal (ATM: 67; SUF: − 89 $W\ m^{-2}$) monsoon scenarios. The lower atmosphere heating rates during 2009 monsoon was also recorded to be as high as 2.9 K day^{-1} in comparison to 2010 (1.7 K day^{-1}) and 2011 (1.9 K day^{-1}). Such findings provide meaningful outcomes in terms of climatic effects of BC aerosols and their associated inference on Indian summer monsoon.

Capsule: BC induced aerosol radiative forcing during 2009 drought year was higher in comparison to deficit (2010) and normal (2011) monsoon scenarios over middle IGP.

* Corresponding author.
E-mail addresses: tb.iesd@bhu.ac.in, tirthankaronline@gmail.com (T. Banerjee).

http://dx.doi.org/10.1016/j.jaerosci.2017.07.016
Received 8 September 2016; Received in revised form 27 March 2017; Accepted 31 July 2017
Available online 01 August 2017

1. Introduction

Black carbon (BC), commonly referred as soot particle, is an integral part of combustion process and contributes significantly in absorbing visible solar radiation and thereby, pose potential in affecting thermal structure of atmosphere (Wang, 2004). The BC potentially modify the atmospheric stability within the boundary layer and free troposphere (Babu et al., 2011). It may also extend from surface to higher elevation, induce significant heating in mid-troposphere and perturbs large-scale modulations in atmospheric circulation (Lee & Kim, 2010). On the contrary, BC also induce strong extinction of solar radiation and thereby, leads to a reduction of insolation, and exhort a very complicated effect on regional hydrological cycle. Besides its direct role in atmospheric heating, there are experimental evidences of its indirect effects on modifying cloud microphysical properties and residence time. Aerosols could alter cloud properties both by microphysical interactions as well as on a more macroscopic scale including entire cloud systems. Aerosol-cloud interactions contribute single largest uncertainty in estimating Earth's energy budget by inducing rapid adjustment in aerosol-cloud-radiation interaction (Myhre et al., 2013). BC embedded in cloud droplets increases its potential absorption which simultaneously affects dissipation of cloud (Bond et al., 2013), while cloud cover is also expected to reduce in presence of BC embedded in the cloud layer (Koren, Kaufman, Remer, & Martins, 2004). Therefore, BC induced modification in atmospheric stability affects global atmospheric circulation and the hydrological cycle, which is often considered as a major challenge for 21st century.

The global BC emission has raised from 8 Tg Cyr^{-1} to 17 Tg Cyr^{-1} (Bond et al., 2004, 2013) with consequent amplifications in its global mean radiative forcing from + 0.20 (IPCC, 2007) to + 0.40 W m^{-2} (IPCC, 2014). These multi wavelength light absorbing particles (Bond et al., 2013) of primary origin are emitted through incomplete combustion of fossil fuels, biomass/ wildfire and aircraft emissions. However, the BC emission vary greatly depending on the source strength. Nearly 60–80% of BC emission in Asian and African countries are contributed through coal and biomass burning while the scenarios in European countries is mostly dominated by automobiles (nearly 70%, Sanap & Pandithurai, 2015). The global budget of BC is contributed by the emissions from combustion of fossil fuels (38%), biofuels (20%), and open biomass burning (42%) (Bond et al., 2004). The BC emissions and its climatic effects are reported throughout the globe, but more extensively over few regional hotspots (e.g. Indo-Gangetic Plain, Eastern China; South-East Asia); regions affected by its trans-boundary movements (e.g. Arctic region) or due to the auxiliary effects of both (e.g. South-East Asia). Trans-boundary movement of BC facilitated by atmospheric circulation is attributed to their finer size and higher atmospheric life time (7–10 days) relative to other short-lived pollutants. The presence of BC aerosols even in pristine regions i.e. Svalbard Arctic Circle (Raju, Safai, Sonbawne, & Naidu, 2015) and Himalaya (Sarkar, Chatterjee, Singh, Ghosh, & Raha, 2015) emphasizes the role of its long range transport. The contributions of Asian region in the global BC budget have often been reported largest (Lamarque et al., 2010). However, scientific understanding on BC emissions and its climatic effects over Asia still consist large uncertainties, mainly due to availability of proper ground monitoring network.

Several hypotheses on the impacts of aerosols on Indian summer monsoon have been given with varying degrees of certainties. Lau and Kim (2006) emphasized the role of absorbing aerosols in enhancing premonsoon rainfall, and its reduction in monsoon period due to enhanced local meridional circulation. Lau, Kim, and Kim (2006) hypothesized that the absorbing aerosols (e.g. BC) can combine with mineral dust and increase the meridional temperature gradient, which further contribute to increased rainfall both during the pre- and summer monsoon. Ramanathan et al. (2005) using a global coupled climate model, recognized the implications of BC aerosols in reducing sea-surface temperature and thereby, reducing monsoonal rain over Indian subcontinent. Meehl, Arblaster, and Collins (2008) by twentieth-century simulations using BC aerosols in a global coupled climate model, hypothesized increased meridional tropospheric temperature gradient in the premonsoon months, which possibly contribute enhanced precipitation over India. However, during monsoon, the contribution of BC aerosols was reported to be negative. Bollasina, Nigam, and Lau (2008) speculated anomalous aerosol loading in late spring, which leads to large-scale variations in the evolution of monsoon over South Asia. Presence of massive aerosols during premonsoon lead to a decrease in cloudiness, thereby reduction in precipitation, increase in shortwave radiation at the surface, and subsequent heating of the ground. Overall, the effects of absorbing aerosols on monsoon was reported to be negative over much of the subcontinent. The contribution of active monsoon breaks (Manoj, Devara, Safai, & Goswami, 2010) characterized by higher anthropogenic aerosols can further modify the summer monsoon and augment the precipitation. In addition to the major source regions, the impacts of BC aerosols can also be extended to other areas and can influence precipitation and sea surface temperature (Wang, 2007). Recently, there are evidences of positive implications of local and remote absorbing dust aerosols (especially from Middle-East Asia) on Indian summer monsoon (Jin, Wei, & Yang, 2014; Jin, Wei, Yang, Pu, & Huang, 2015), while the degree of response is projected to be highly sensitive to the absorbing abilities of aerosols (Jin, Yang, & Wei, 2016). Using a high-resolution regional climate model coupled with online chemistry, Jin et al. (2016) concluded both the magnitude and direction of dust-induced monsoon rainfall changes are highly sensitive to aerosol absorptive properties, as dust aerosols with stronger absorption can result in larger increases of the monsoonal rainfall.

India contributes (0.41 Tg (BC)yr^{-1}) substantial proportion of global BC emission (8 Tg yr^{-1}, Bond et al., 2004) with a variety of sources based on different land-use pattern, burning of biofuels (0.17 Tg (BC)yr^{-1}), open biomass (0.14 Tg (BC)yr^{-1}) and fossil fuel (0.10 Tg (BC)yr^{-1}) (Venkataraman, Habib Fernandez, Miguel, & Friedlander, 2005). The explicit use of conventional fuels and less efficient combustion technologies in rural India contribute maximum BC emissions (Banerjee, Kumar, Mall, & Singh, 2017; Venkataraman et al., 2005). Despite of such huge burden, their associated impacts on precipitation and monsoon or vice-versa are sparsely documented. For the present submission, efforts are made to identify the impact of normal and drought monsoon scenarios on regional BC concentrations and associated radiative impacts for a typical urban station over middle-IGP. We have investigated both the diurnal and inter-annual variations of BC for different monsoon scenarios to recognize its radiative effects and its potential to modify the atmospheric thermal structure within the boundary layer. Note that, we have only investigated the radiative impacts of BC over different monsoon scenarios, but have not considered any microphysical effects of BC aerosols on the formation of cloud and

dynamics of Indian summer monsoon. The implications of such analysis may be many with potential applications in various climate models and for forecasting Indian summer monsoon under varying BC emission scenarios.

2. Experimental methods

2.1. Site description

The study site Varanasi (25°28′N and 82°96′E; 82.2 m AMSL) represents an urban environmental set up over middle-IGP, characterized by multiple sources of aerosol inflow predominately from road dust re-suspension, commercial activities, vehicular exhausts and biomass/waste burning (Kumar et al., 2016; Murari, Kumar, Mhawish, Barman, & Banerjee, 2017). The region experiences a humid sub-tropical climate with distinct seasonal variations. Seasonal distinction over the study site include hot and dry summer (March to June, 38–42 °C), intense rainfall during monsoons (June to September, 1100 mm annual rainfall, 80% of which occurs during monsoon) and cold during winters (December to February, 7–15 °C). The climate of the study area is usually affected by a wide range of synoptic weather phenomena however, with minimal localized effects of oceans and mountains (Murari, Kumar, Singh, Singh, & Banerjee, 2016; Murari et al., 2017).

2.2. Ground based measurements

2.2.1. BC mass loading

The continuous and real time measurements of BC mass concentrations at the study site were made using a 7-channel Aethalometer (AE 42, Magee Scientific, USA). The principle of estimation of BC aerosols through Aethalometer is based on the attenuation of a beam of light by deposited aerosols on the filter. The Aethalometer measures attenuation at seven different wavelengths (370, 470, 520, 590, 660, 880 and 950 nm). However, values corresponding to 880 nm are considered for BC aerosols based on its maximum absorption capacity. The estimation of BC concentration by Aethalometer is based on the assumption that the increase in attenuation of light (ATN) by aerosols is solely due to light absorption by BC accumulated on the filter. The rate of change of light attenuation is used to calculate BC. Further details of the operating principle and calculation of BC may be found in the works of Hansen, Rosen, and Novakov (1984). An absorption efficiency of 16.6 $m^2\ g^{-1}$ (provided by the manufacturer) was used to estimate the BC mass loadings.

The Aethalometer measured BC mass concentrations are subject to under estimation due to the non-linearity that may arise due to high deposition of BC on filter tapes (loading or shadowing effect). This loading effect was removed by using a correction algorithm as proposed by Virkkula et al. (2007). As the information regarding scattering coefficient was not available, the corrected attenuation coefficient can be expressed as:

$$b_{ATN}(\text{corrected}) = (1 + k^{*}\text{ATN})^{*}\, b_{ATN}(\text{Aethalometer}) \quad (1)$$

The corrected BC concentration can be expressed as

$$\text{BC (corrected)} = b_{ATN}(\text{corrected})/\sigma_{ATN} = (1 + k^{*}\text{ATN})^{*}\text{BC (Aethalometer)} \quad (2)$$

where, 'b_{ATN}' is the attenuation coefficient, 'ATN' is the attenuation value from Aethalometer, 'k' is the compensation parameter and 'BC' is the Black Carbon mass concentration in ng m^{-3}. The compensation parameter 'k' varies widely with change in sampling locations, season, composition and age of aerosols (Hansen et al., 1984). The linear fit of BC mass concentrations and optical attenuation (ATN) was plotted and used for the calculation of 'k' value (Safai, Raju, Budhavant, Rao, & Devara, 2013).

2.2.2. Particulate mass loading and micro-meteorology

Particulates with aerodynamic diameter ≤ 10 μm (PM_{10}) were monitored at Banaras Hindu University (BHU) campus during monsoon months (JJAS, June to September) from year 2009 to 2011, on weekly basis. The 24-h average PM_{10} samples were collected on glass microfiber filters (GF/A, Whatman; 47-mm diameter) using particulate sampler (APM-550, Envirotech) with size selective inlet at a flow rate of 1 $m^3\ h^{-1}$ (accuracy ± 2%). Filters were pre-conditioned in a desiccator with controlled humidity conditions and weighed before and after sampling using a microbalance (AY220, Shimadzu). Details of particulate monitoring procedure can be found in the works of Murari et al. (2017) and Kumar et al. (2016). The daily averaged micro-meteorological parameters e.g. temperature, relative humidity (RH) and wind speed were obtained from wunderground.com, a web based meteorological database which provides a range of meteorological variables for a particular geographical area. The monthly average rainfall for monsoon seasons were obtained from regional India Meteorological Department station, located within the University campus.

2.3. Satellite based measurements

Satellite based columnar AOD were retrieved from Terra MODIS atmosphere level 2 product. An area within 25°10′37″–25°19′47″N and 82°54′7″ − 83°4′30″E, uniformly surrounding the ground monitoring site was specifically selected to retrieve MODIS-AOD at 550 nm. Terra MODIS 3-km atmospheric product (MOD04_3K; MODIS collection 6) was retrieved through Atmosphere Archive and Distribution System (http://ladsweb.nascom.nasa.gov), averaged in pre-selected grid, screened for cloud cover and further used for analysis (Kumar, Tiwari, Murari, Singh, & Banerjee, 2015; Kumar et al., 2017). Single scattering albedo (SSA) at 550 nm (level 3, 0.25° × 0.25°) and total columnar ozone (TCO, level 3e, 0.25° × 0.25°) were retrieved from Ozone

Monitoring Instrument (OMI) on board Aura satellite. It is important to recognize that the different orbital path of MODIS-Terra (descending node 10.30 a.m. local time) and OMI-Aura (descending node 1.30 p.m. local time) do not instigate additional uncertainties in to the measurements. This is especially because measurement of TCO and SSA over a particular geographic point are function of seasons, and in most of the cases, do not change on hourly basis. Shukla, Srivastava, Banerjee, and Aneja (2017) compared the daily and satellite overpass time-averaged TCO concentrations over Varanasi and reported insignificant daytime variations. In an identical condition, AOD may vary in a shorter time frame, especially due to influence of local wind, but such uncertainties in AOD measurement are included within the overall estimation of uncertainty level for radiative transfer model. The predicted retrieval uncertainty of MODIS-derived AODs was 0.05 ± 0.15 over land and 0.03 ± 0.05 over ocean (Remer et al., 2005). Total Columnar Ozone level 3e global data (OMDOAO3e, Version 003) gridded at 0.25°×0.25° were retrieved using Differential Optical Absorption Spectroscopy (OMIDOAS) algorithm (Kumar et al., 2017) from NASA Goddard Earth Sciences Data and Information Service Centre (http://www.esrl.noaa.gov/). The columnar water vapor (CWV) content was retrieved from Modern-Era Retrospective Analysis for Research and Applications (MERRA) level 3 data gridded data with resolution of 0.5° latitude and 0.67° longitude.

2.4. Particle backward trajectory

NOAA HYSPLIT (Hybrid Single Particle Lagrangian Integrated Trajectory) backward trajectory model (Draxler & Rolph, 2003) was used to understand trans-boundary movement of air mass over the entire region (5–40°N, 30–100°E). Particle back trajectories were plotted based on archived data set at an altitude of 125 m (AMSL), to predict 7-days air mass back-trajectories for each year only for monsoon. In a similar condition, particle backward trajectories were also simulated for very high and low BC loading days (30 days) within entire BC monitoring period from 2009 to 2011, to distinguish any specific movement of air mass which were influencing regional BC loading.

2.5. Aerosol optical properties and radiative forcing

Water soluble (30% of total PM_{10}) and water insoluble (70% of total PM_{10}) aerosol mass loading were introduced along with BC mass concentration in the OPAC (Optical Properties of Aerosol and Cloud) model to obtain optical properties of aerosol such as AOD, SSA and asymmetric parameter (ASP) (Hess, Koepke, & Schult, 1998). The mass concentrations of aerosols were then converted to number densities of water soluble (WS), water insoluble (WIS) and BC (soot) components from which the optical properties were derived. The AOD and SSA were reconstructed in a way until the modelled and satellite derived values matched within ± 5% deviation. The optical parameters were estimated at different wavelengths in spectral range of 0.2–4.0 μm. The OPAC-derived AODs were validated with those with Terra MODIS-AOD.

The OPAC derived optical parameters were used in Santa Barbara DISORT Atmospheric Radiative Transfer (SBDART) model for radiative forcing estimation during different monsoon scenarios from 2009 to 2011. The SBDART includes multiple scattering in a vertically inhomogeneous, non-isothermal plane-parallel media and efficient enough in resolving radiative transfer equation (Ricchiazzi, Yang, Gautier, & Sowle, 1998). The monthly mean values of AOD, SSA, ASP, CWV, TCO, Visibility and α were included as input for SBDART. This algorithm includes multiple scattering in a vertically inhomogeneous, non-isothermal plane-parallel media, and is shown to be computationally efficient in reliably resolving the radiative transfer equation. The short-wave aerosol radiative forcing (ARF) were calculated using 10 solar zenith angles starting from 0 to 89 with increment of 10 and proceed for both conditions i.e. with aerosols and without aerosols, at 33 atmospheric layers with 90% RH level (Raju et al., 2016). The surface albedo used for the study was a combination of snow, ocean, sand and vegetation. The fraction values regarding surface albedo were decided on visual observation considering the prevailing conditions in ground monitoring station. The overall uncertainty in the estimated daily ARF due to deviations in simulation by SBDART was in the range of 10–15% (Alam, Trautmann, & Blaschke, 2012). The average forcing for surface (SUF) and top of the atmosphere (TOA) were estimated separately for composite aerosols and atmospheric forcing (ATM) was calculated as the difference between two.

The ARF over atmosphere (ATM) was also used to compute atmospheric heating rate (K day^{-1}). Aerosol induced atmospheric heating rate (∂T/∂t) was calculated using Eq. (1′):

$$\partial T/\partial t = (g/Cp)*(\Delta F/\Delta P) \quad (1')$$

where ΔP is the pressure difference between top and bottom boundary layer, *Cp* is specific heat capacity of air at constant pressure and *g* is the acceleration due to gravity. Atmospheric heating rate was computed for the complete atmospheric column considering variation between aerosol-induced and an aerosol-free atmosphere.

3. Results and discussion

3.1. Characteristic of monsoon precipitation and aerosol loading

The possible repercussion of aerosol induced climate change on Indian summer monsoon (southwest monsoon) is highly uncertain. Indian summer monsoon is inconsistent with number of factors that essentially regulate its extent and strength. Inconsistent pattern of monsoon rainfall was observed from 2009 to 2011 throughout Indian sub-continent, with severe drought during 2009, a partly deficit monsoon during 2010 and a normal monsoon during 2011 (Fig. 1). During 2009 drought year, all India area weighted rainfall was 698.1 mm, with a deficiency as a whole of − 22% from long period average (LPA for 1901–2009: 892.2 mm; imd.gov.in).

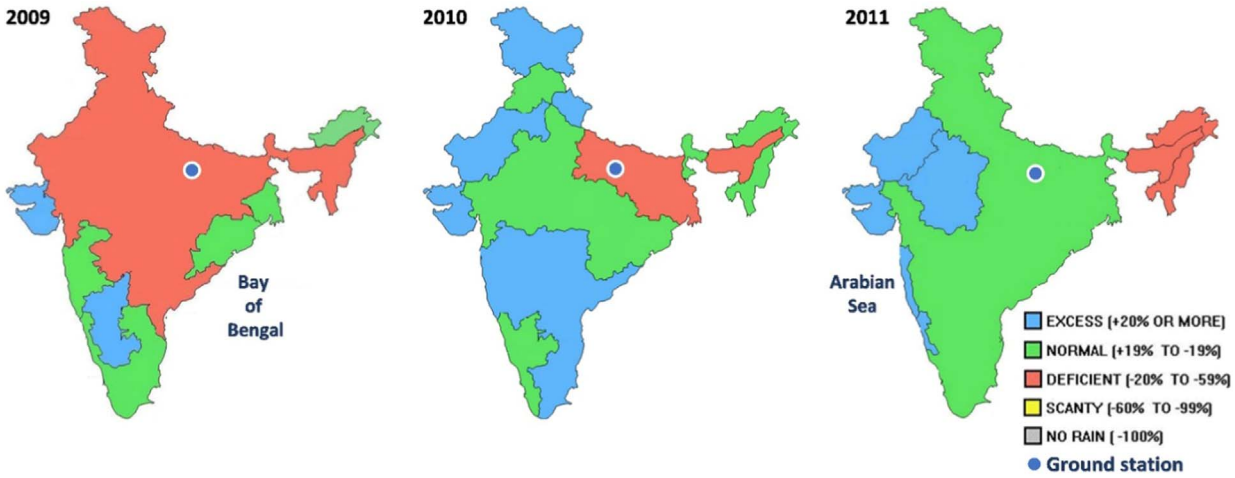

Fig. 1. Scenarios of Indian summer monsoon from 2009 to 2011. Note:Modified from IMD monsoon page, http://www.imd.gov.in/pages/monsoon_main.php.

This was the third highest deficient summer monsoon all over India closely followed by 1918 and 1972. Subsequently, monsoon rainfall appeared to be normal during 2010 with season specific average rainfall of 910.6 mm having 2% departure from LPA. However, parts of India (mostly over middle to lower IGP, Fig. 1) still experienced a deficient monsoon (− 20 to − 59%) during 2010. Additionally, 2010 monsoon accounted various anomalous rainfall and wind circulation features, which necessitate further investigation. In 2011, summer monsoon appeared to be normal (901.2 mm, 2% departure from LPA) with monsoon reported to be strongly influenced by moderate La Niña event. Although, entire country experienced a relatively well distributed monsoonal rainfall but, northeast India experienced a deficit rain during 2011 (Monsoon page, imd.gov.in). Monsoonal rainfall characteristics in ground monitoring station at Varanasi resemble the country-wide trend with minimum rainfall during 2009 (total monsoon rain: 437.3 mm), partly deficit rainfall during 2010 (rain: 613.4 mm) and normal monsoon during 2011 (total monsoon rain: 1207.0 mm). Fig. 2 represent TRMM (Tropical Rainfall Measuring Mission) retrieved daily rainfall pattern during JJAS months from 2009 to 2011. It establishes the significant variation of spatial distribution of monsoonal rain with minimum rainfall over western provinces of India during 2009 drought. Rainfall was also deficient over Central Highlands, parts of Deccan Plateau (during 2009) which gradually increases in 2010, before reaching to a normal during 2011.

The spatio-temporal distribution of airborne particulates over entire Indian sub-continent was analysed for monsoon (Fig. 3). The region experiences characteristic variation in aerosols loading with presence of diverse aerosol types (Sen et al., 2016; Sen, Abdelmaksoud, Nazeer Ahammed, Alghamdi, & Banerjee, 2017; Singh, Murari, Kumar, Barman, & Banerjee, 2017a). Monsoon specific spatial distribution of columnar aerosol properties (AOD and FMF, fine mode fraction) was analysed using Terra MODIS Level 2 daily aerosol product and plotted in Fig. 3. Aerosols fine mode fractions represent an estimate of fine particulates' contribution (mainly of anthropogenic origin) to the total optical depth. Over the entire IGP, comparably high AOD values were observed from

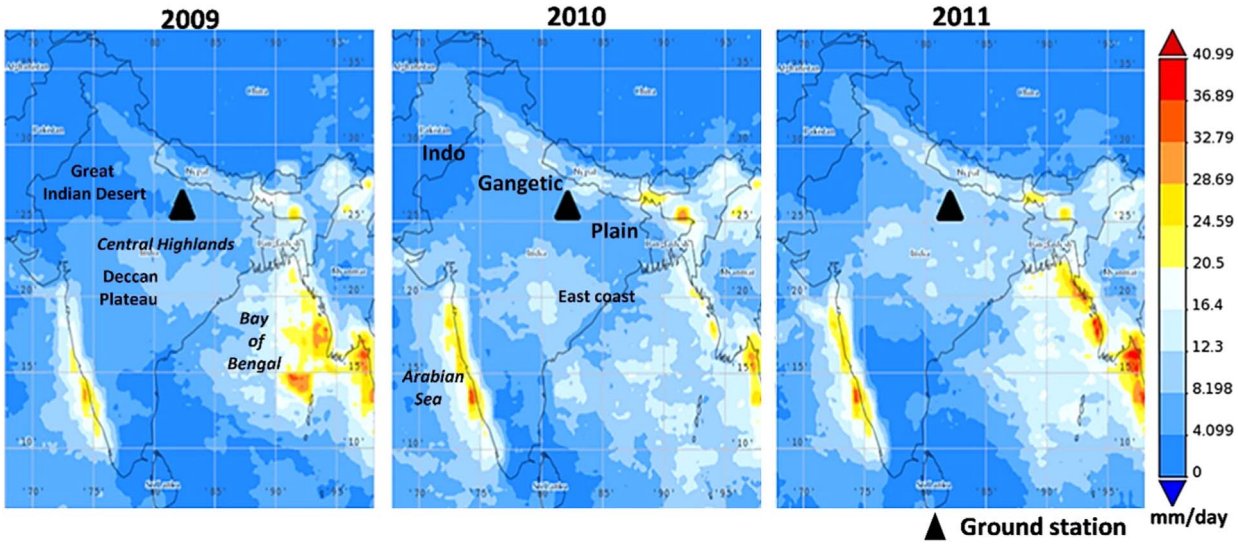

Fig. 2. Variation of TRMM retrieved monsoon rainfall from 2009 to 2011.

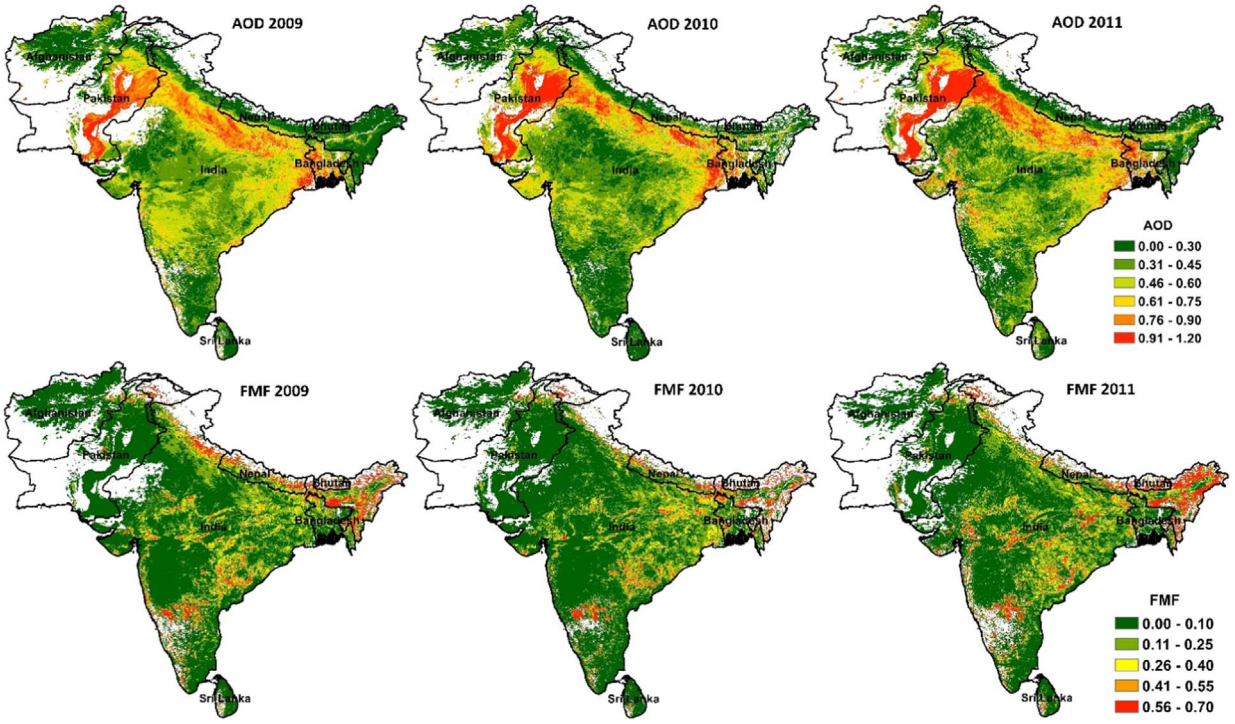

Fig. 3. Variation of Terra MODIS AOD and FMF during monsoon from 2009 to 2011.

2009 to 2011 (Fig. 3). The high aerosol loading (1.03 ± 0.15) during typical monsoon period of 2009 was possibly due to prevailing drought condition which facilitate generation of wind-blown crustal dust. Interestingly, it was during 2009 and 2010 monsoon (1.07 ± 0.53), aerosol columnar aerosol loading over Varanasi transect was significantly high before being reduced in 2011 (0.89 ± 0.20). Both 2009 and 2010 monsoon also recorded a 10% increase in columnar aerosol loading in comparison to 10 year's average AOD (0.90; 2006–2015) over Varanasi transect, while aerosol loading during 2010 were 2% lower compared to 10-years average. Over the entire geographical region, wind-blown crustal materials are often considered to be the most dominating particulate source

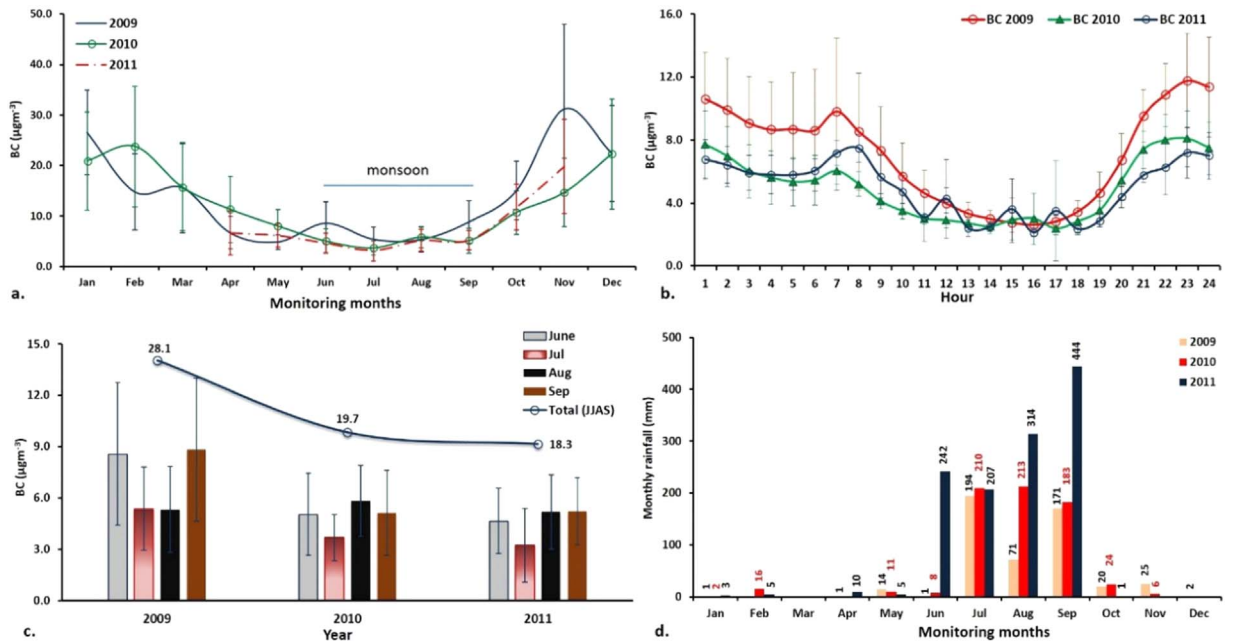

Fig. 4. Black carbon mass loading in Varanasi from 2009 to 2011 (a) variation of monthly means, (b) diurnal variations during monsoon, (c) variation of monthly means during monsoon, and (d) monthly variations of rainfall.

(Banerjee, Murari, Kumar, & Raju, 2015; Singh et al., 2017a). Additionally, contribution of trans-boundary aerosols from north-western dry region contributes significantly to total aerosol loading (Kumar et al., 2015; Sen et al., 2016, 2017). Dust aerosols mostly originate from western dry regions of India (like Great Indian desert), Pakistan and Afghanistan, and from Middle-East Asia, contribute huge particulate mass during premonsoon, mostly dominated by coarser particulates. Fig. 3 FMF image also indicates the dominance of coarser particulates over entire IGP during 2009–10 while slight increase in finer particulates during 2009. These coarser particulate are mostly composed of mineral species and often coated with Sulphur, mainly induced by chemical reactions at its surface (Murari et al., 2016). In general, these particles act as giant cloud condensation nuclei (CCN) and enhance the possibilities of collision and coalescence of cloud droplets and thereby, increase formation of warm precipitation (Rosenfeld, Rudich, & Lahav, 2001). In contrast, presence of incremental amount of particulates possibly induce formation of shallow cloud cover, decrease cloud droplet size, and thereby, reduce/delay in rainfall. The CCN under favorable meteorological conditions may therefore, help in the formation of clouds dominated by small droplets but having low coalescence efficiencies, which ultimately reduce the amount of precipitation (Rosenfeld et al., 2001; Singh, Mhawish, Deboudt, Singh & Banerjee, 2017b).

3.2. Variation of BC mass concentration

Fig. 4 represents the variation of BC loading throughout the monitoring period in Varanasi (Fig. 4a), coupled with variation in monsoon specific diurnal (Fig. 4b) and monthly BC means (Fig. 4c), and monthly rainfall during 2009–2011. BC loading was consistently high during winter (December–February) and minimum during monsoon (June-September). Diurnal variation of BC loading during 2009 drought year expressed a regular decreasing pattern from midnight (0000 h, 11.4 μg m^{-3}) to evening hours (1600 h, 2.6 μg m^{-3}), before being gradually increased around at 2300 h (11.8 μg m^{-3}). Such trend was identical for deficit to normal monsoon years, except an overall decline in BC loading. Two isolated pattern in hourly BC variations was specifically recognized. An early morning hour (0700–0800 h) and late hour peak at 1900–2300 h in BC mass loading coincide with enhanced traffic rush hours. Vehicular emissions are typically considered as most significant contributor of regional BC (Kumar et al., 2017; Murari et al., 2016). Interestingly, a sine variation in diurnal 2011 BC loading at 1100–1800 h was inconsistent to that of 2009 and 2010. Further, in 2010–2011 BC mass loading was minimum (2010: 2.4; 2011: 2.1 μg m^{-3}) during evening hours (1600–1700 h) while maximum (2010: 8.1; 2011: 7.2 μg m^{-3}) only during mid-night (2300 h). The observed diurnal variation of BC is mainly attributed because of the dynamics of atmospheric boundary layer (ABL), while anthropogenic activities possibly instigate the nocturnal BC peak (Fochesatto et al., 2001). Fig. 5 indicates the time-series of daily averaged BC loading in comparison to 3-h average ABL for each corresponding year. The deepening of the ABL during daytime and the associated convective turbulence thoroughly mix and re-distribute aerosols to greater vertical extent, which were otherwise confined in the shallow night-time nocturnal boundary layer. This results in a dilution of BC concentrations near the surface, despite higher contributions through increased vehicular and house-hold activities. Similar discussions on diurnal variation of BC mass concentration have also been reported by many researchers across India (Babu, Nair, Gogoi, & Moorthy, 2015; Kumar et al., 2017) and in polar region (Raju et al., 2015).

To recognize the nature of temporal changes, monthly mean BC values were examined both during drought (2009), deficient (2010) and normal monsoon scenarios (2011, Fig. 4c). Relatively high BC mass loading were measured during drought year (2009, mean ± SD: 7.0 ± 3.3; range: 5.3–8.8 μg m^{-3}) in contrast to 2010 (mean: 4.9 ± 2.1, 3.7–5.8 μg m^{-3}) and 2011 (mean: 4.6 ± 2.1, 3.2–5.2 μg m^{-3}). Interestingly, intra-monsoonal BC variation was relatively less in 2010 and 2011, despite of having reasonable changes in rainfall pattern.

3.3. Source characterization and micro-meteorology

In order to investigate the possible origin and trans-boundary movement of aerosols, seven days air-mass back trajectories at an altitude of 125 m (AMSL) over Varanasi were projected using NOAA-HYSPLIT and represented in Fig. 6. The mainland station Varanasi is located at the eastern end of IGP, and the prevailing westerly/southwesterly travelling from Arabian Sea and from parts of Indian subcontinent contribute both marine as well as crustal air mass to the station (Kumar et al., 2017; Sen et al., 2017). Thus, the synoptic meteorology and local ABL dynamics play a crucial role in regulating temporal variations of the surface BC concentrations. Back trajectory analysis revealed that both marine and continental air mass simultaneously contributed to total aerosol loading over middle-IGP. Marine air masses both from Arabian Sea and Bay of Bengal were found contributing to the region, in continuation to

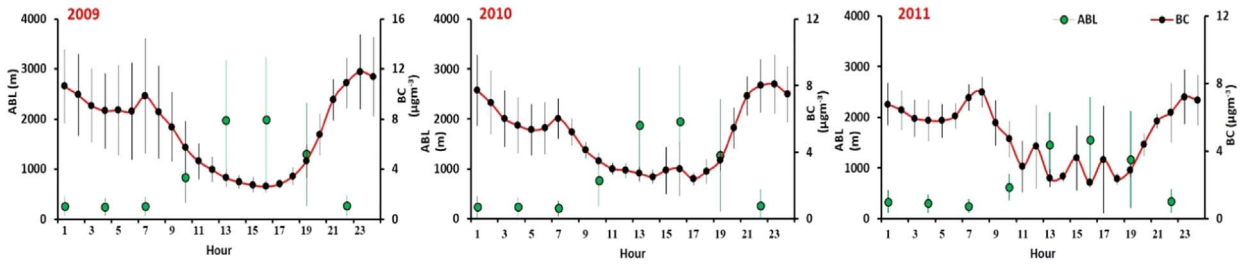

Fig. 5. Hourly variation of black carbon during monsoon with respect to atmospheric boundary layer. Note: BC variations are in 1 h duration while ABL is averaged over 3 h.

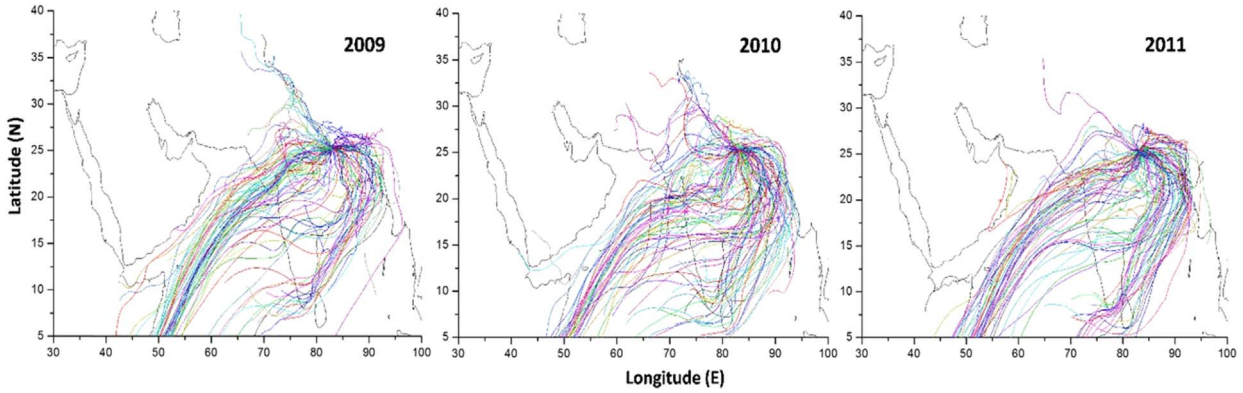

Fig. 6. HYSPLIT seven-days backward trajectories during monsoon from 2009 to 2011.

continental air mass primarily from Central highlands, Deccan Plateau and southern peninsular region of Indian sub-continent. However, no such temporal differences in air mass trajectories were evident over the period. In continuation of identifying trans-boundary movement of airborne particulates by prevailing air mass for entire monsoon, emphases were also made in recognizing the movement of air mass especially during very high and low BC loading days. This has been continued with identifying 30 highest and lowest 24-h mean BC loading days within entire BC monitoring period from 2009 to 2011. For low BC loading days, there were no characteristic deviation of general pathways of air mass transport as shown in Fig. 7. In contrast, during high BC loading days, there were few instances of origin and transport of air masses especially from upper IGP e.g. northern parts of Pakistan, Punjab (India) and western semi-arid region, which possibly contributed to higher BC loading over the ground-station. Further, this has been more prominent during 2009 and 2010, when both AOD and BC loading were considerably high compared to 2011. This certainly indicates the additional contribution of aerosols emitting sources over upper IGP and western dry regions in influencing aerosol loading and chemistry in the lower IGP.

Meteorological parameters such as ambient temperature (°C), relative humidity (%), wind speed (m/s) and rainfall (mm) play a vital role in assessing background condition of the observational station and therefore, were simultaneously measured and plotted in Fig. 8. Rainfall pattern clearly distinguish the drought, deficit and normal monsoon scenarios (Fig. 8a). The 2009 southwest monsoon recorded as the third highest deficient Indian summer monsoon for the period of 1901–2009 (Tyagi, Hatwar, & Pai, 2010). During 2009 monsoon, Varanasi received an average monthly rainfall of 109.3 mm (total monsoon rain: 437.3 mm) which was significantly lower than the monsoon scenarios prevailed during 2010 (monthly avg.: 153.4; monsoon rain: 613.4 mm) and 2011 (monthly avg.: 301.8; monsoon rain: 1207.0 mm). Accordingly, relative humidity shows gradual increase from June reaching to a peak during August for 2010-11 monsoon, while during September for 2009 drought year (Fig. 8b). There is a negative correlation between temperature and relative humidity ($R = -0.98$) for the entire period. Comparably high wind speed persisted initially in monsoonal months before gradually declined till the end of season (Fig. 8c). Ambient temperature also reduced gradually from June to September in each year.

3.4. Comparison between observed and modelled AOD and SSA

The aerosol optical properties (AOD, SSA and ASP) each at 550 nm and Angstrom Exponent were computed by OPAC model at

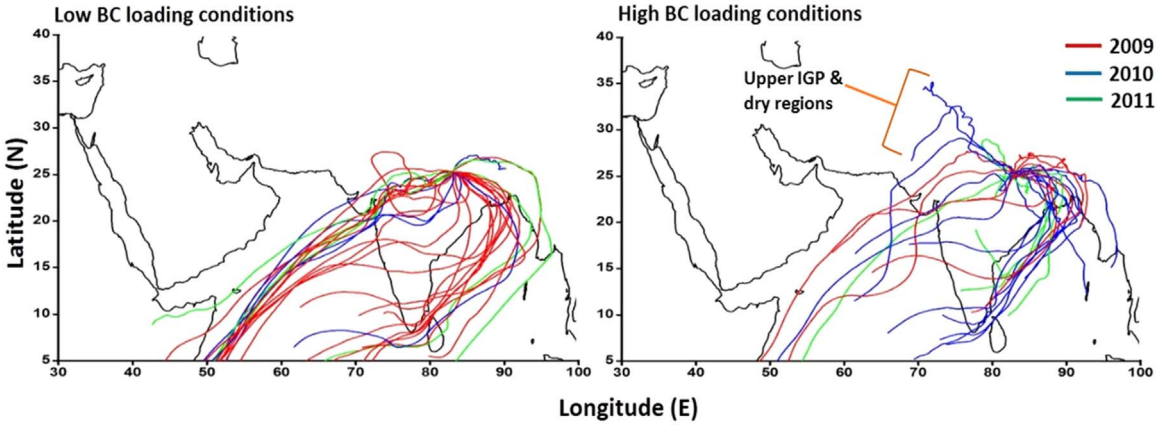

Fig. 7. HYSPLIT seven-days backward trajectories for very high and low BC loading days.

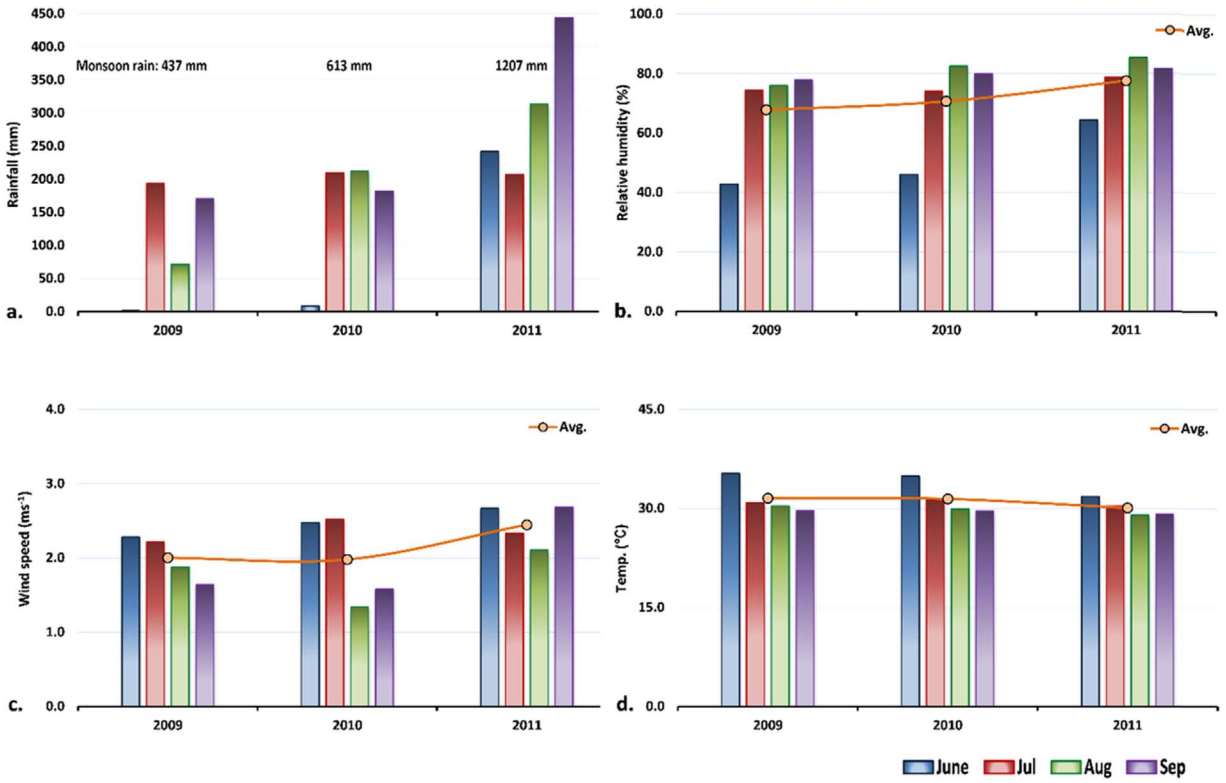

Fig. 8. Variation of meteorological variables during monsoon from 2009 to 2011.

90% RH, using PM_{10} chemical composition and BC mass loading. The comparison of OPAC derived AOD and SSA for composite aerosols at mid-visible wavelength (0.55 μm) and those obtained from satellite based data are shown in Fig. 9. The OPAC derived AOD and SSA are fine tuned to match closely with satellite derived parameters. There was no such variation in satellite retrieved SSA (mean ± SD: 0.99 ± 0.03; range: 0.9–1.0) within the monsoon throughout 2009–2011, and the mean difference between satellite retrieved and OPAC derived SSA was 0.07. In absence of ground measurement, AOD was derived from the OPAC (0.2–4.0 μm) considering aerosol chemical composition, and further compared with satellite retrieved AOD. Both OPAC modelled and satellite retrieved AOD were almost identical with mean difference between these two products were 0.004. For each individual year, OPAC modelled AOD was slightly higher till July (2009: 1.2, 2010: 1.7, 2011: 1.1) before being gradually declined till the end of the monsoon. However, such decline was characteristically higher during normal and deficit monsoons in contrast to drought year. The SSA was found to be within 0.89–0.95 over the ground station while both satellite retrieved and model derived SSA were reciprocating each other.

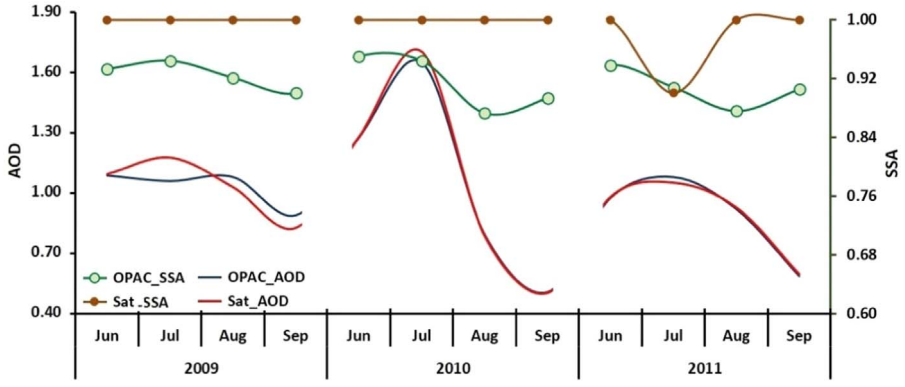

Fig. 9. Comparison of modelled and satellite retrieved AOD and SSA.

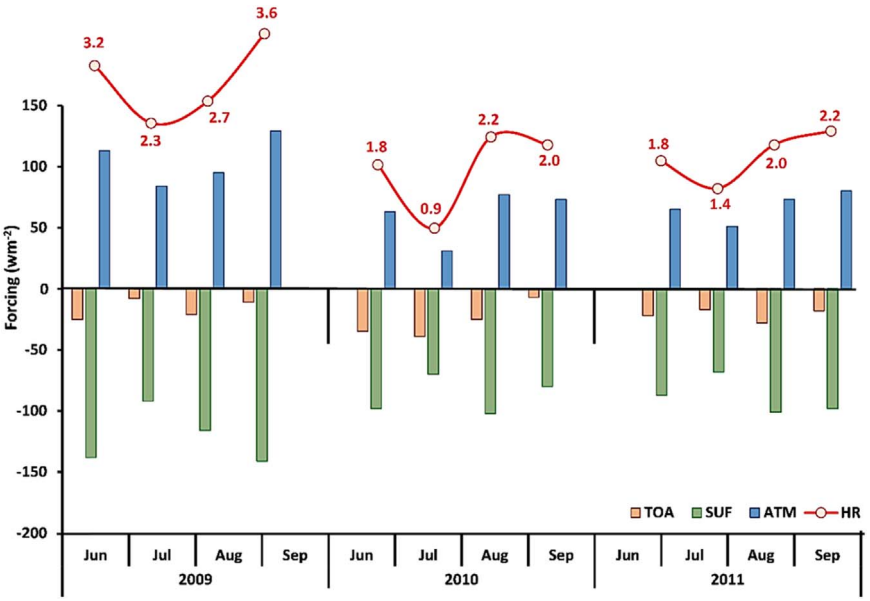

Fig. 10. Estimate of radiative forcing (W m^{-2}) and heating rate (K day^{-1}) during monsoon from 2009 to 2011.

3.5. Aerosol radiative forcing and heating rate

The OPAC derived AOD, SSA, ASP and α were simultaneously used coupled with satellite retrieved TCO, CWV and visibility as an input in SBDART, to compute aerosol direct radiative forcing in the spectral range of 0.2–4.0 μm. For the present analysis, aerosol radiative forcing has been computed for 2009–2011, 2009-2011 monsoon seasons considering composite aerosol conditions at the surface (SUF), top of the atmosphere (TOA) and atmosphere (ATM).

Fig. 10 revealed positive forcing (warming effect) at ATM while negative forcing (cooling effect) both at TOA and SUF, throughout the monsoon period from 2009 to 2011. During 2009 drought year, very high ATM forcing with monthly mean of 105 W m^{-2} was evident, which was exceptionally high in contrast to normal monsoon scenario of 2011 (67 W m^{-2}). In 2010, the ATM forcing (61 W m^{-2}) was substantially low compared to drought year while being much comparable to that of 2011. Identically, aerosol induced SUF radiative forcing (− 122 W m^{-2}) was also high during 2009 drought year in comparison to 2010 (− 88 W m^{-2}) and 2011 (− 89 W m^{-2}). The TOA forcing during 2009 drought (− 16 W m^{-2}) was somewhat lesser in comparison to 2010 (− 27 W m^{-2}) and 2011 (− 21 W m^{-2}). Therefore, greater implication of aerosol induced radiative forcing was only evident during 2009 drought year both at atmosphere (warming) and surface (cooling), while its inference was relatively less at top of the atmosphere (cooling). This definitely indicate the larger implications of atmospheric aerosols, especially absorbing aerosols like BC in regulating thermal structure of the atmosphere by inducing additional heat to the environment. Presence of absorbing aerosols at lower atmosphere absorb solar radiation and thereby, reduces the solar radiation reaching the Earth's surface. More often these absorbing aerosols coupled with other aerosols particularly sulphates, provide nuclei for cloud droplets and ice crystals, potentially increasing the number of small cloud drops and ice crystals. These ice crystals coalesce very inefficiently into rain drops resulting reduction in total rainfall (Ramanathan, Crutzen, Kiehl, & Rosenfeld, 2001).

The observations well validate the initial argument that higher BC aerosol loading in the atmosphere leads to high ATM (warming effect) and SUF forcing (cooling effect), while its forcing implications are more positive in upper atmosphere (positive TOA forcing). Table 1 compares the BC loading with corresponding ATM forcing over India specifically during pre-, post- and for typical monsoon scenario. During 2009 drought year, monsoon specific heating rate in the lower atmosphere was found to be as high as 2.9 K day^{-1} in comparison to normal monsoon scenarios of 2010 (1.7 K day^{-1}) and 2011 (1.9 K day^{-1}). This clearly indicates the considerable influence of absorbing BC aerosols for inducing additional heat to lower atmosphere over middle-IGP, particularly during drought year.

Conclusively, based on the evidences it may be stated that, BC induced aerosols radiative forcing induce strong atmospheric absorption of incident solar radiation which alter atmospheric thermodynamics and simultaneously regional atmospheric circulation over middle-IGP. However, the influence of direct and indirect effects of various aerosol species on Indian summer monsoon pose multiple uncertainties and require intensive scientific research for better understanding.

3.6. Conclusions

The ground-monitored aerosol loading and BC mass concentration measured in Varanasi over middle IGP, are analysed especially for three typical monsoon scenarios from 2009 to 2011. The radiative effects of composite aerosols at short wavelength have been estimated considering measured BC mass concentrations and satellite retrieved aerosol optical properties. Also, the impact of

Table 1
Variation of BC mass loading and ATM radiative forcing during Pre/Post-monsoon period.

Station	Period	BC (μg/m^3)	ATM Forcing (W/m^2)	Reference
Ahemdabad	Monsoon, 2008	2.1 ± 0.8	33.6	Ramachandran and Kedia (2010)
Ahemdabad	Pre-Monsoon, 2007	1.8	33.7	Das and Jayaraman (2011)
Dibrugarh	Monsoon, 2008	3.4 ± 0.9	32.2	Pathak, Kalita, Bhuyan, Bhuyan, and Moorthy (2010)
Goa	Monsoon, 2008	0.7	7.29	Menon et al. (2014)
Trivandrum	Monsoon (Multiyear Measurements)	1.2	25.5	Babu, Moorthy, and Satheesh (2007)
Visakhapatnam	Monsoon, 2006	1.7	12.20	Sreekanth, Niranjan, and Madhavan (2007)
Delhi	Post-Monsoon, 2012	Day: 11.66 ± 3.94 Night: 19.44 ± 4.65	43.6–130.9	Bisht et al. (2015)
Delhi	Monsoon, 2010	0.58	23 ± 3.89	Surendran et al. (2013)
Udaipur	Pre-Monsoon, 2007	0.9	20.5	Das and Jayaraman (2011)
Mt. Abu	Pre-Monsoon, 2007	0.7	18.5	
Varanasi	Monsoon, 2009	7.0 ± 3.3	105	This study
	Monsoon, 2010	4.9 ± 2.1	61	
	Monsoon, 2011	4.6 ± 2.1	67	

chemical and optical properties of aerosols on atmospheric heating are studied. The main findings of the investigation are:

1. During 2009, India recorded the third highest deficit in summer monsoon (− 22% of long period average) which gradually improved in 2010 (overall deficit monsoon) before achieving a normal monsoon in 2011. The ground monitoring station in Varanasi over middle-IGP also registered drought during 2009 (monsoon rain: 437.3 mm), a deficit monsoon in 2010 (total rain: 613.4 mm) and normal monsoon in 2011 (monsoon rain: 1207.0 mm).
2. The Terra MODIS retrieved aerosol columnar loading revealed high aerosol optical depth over Varanasi transect, both during 2009 (AOD: 1.03 ± 0.15) and 2010 (AOD: 1.07 ± 0.53) before being reduced during 2011 monsoon (AOD: 0.89 ± 0.20).
3. Surface BC concentration found to be high during winter season (December-February) and low during monsoon period (June-September). The hourly variation of BC revealed a bi-modal distribution with high BC mass concentration during 2009 before being subsided during 2010 and 2011.
4. Air mass responsible for transporting BC and other airborne particulates to ground-station was of both marine and continental origin. However, during high BC loading days, contribution of upper IGP e.g. like northern parts of Pakistan, Punjab (India) and western semi-arid region were recognized especially for 2009 and 2010.
5. Composite aerosol radiative forcing during 2009 drought year was considerably high for ATM and SUF (ATM: 105; SUF: − 122 W m^{-2}) in contrast to 2010 (ATM: 61; SUF: − 88 W m^{-2}) and 2011 monsoon scenarios (ATM: 67; SUF: − 89 W m^{-2}).
6. The lower atmospheric heating rates during 2009 monsoon was found to be as high as 2.9 K day^{-1} in comparison to deficit (1.7 K day^{-1}) and normal monsoon scenarios (1.9 K day^{-1}).
7. Drought specific increase in atmospheric heating rate clearly indicates the considerable influence of absorbing BC aerosols in regulating atmospheric thermal structure, particularly by inducing additional heat to lower atmosphere. Such observation may well be useful in improving regional uncertainties in climate models.

Acknowledgements

Atmospheric black carbon BC was monitored under Aerosol Radiative Forcing over India (ARFI) scheme (Code: P-32-13) financed by Indian Space Research Organization, Thiruvananthapuram. The MODIS-AOD, OMI-O_3 and TRIMM-rainfall are courtesy of NASA's Earth-Sun System Division. Authors also acknowledge aerosol sampling done by S.K. Jayanti and N.T.S. Anil Kumar. Meteorological data were courtesy of IMD-Varanasi and wunderground.com. Authors are thankful to the Director, IESD-BHU and Dean, FESD-BHU for all the support to undertake this work.

References

Alam, K., Trautmann, T., & Blaschke, T. (2012). Aerosol optical and radiative properties during summer and winter seasons over Lahore and Karachi. *Atmospheric Environment*, *50*, 234–245.

Babu, S. S., Moorthy, K. K., Manchanda, R. K., Sinha, P. R., Satheesh, S. K., Vajja, D. P., et al. (2011). Free tropospheric black carbon aerosol measurements using high altitude balloon: Do BC layers build "their own homes" up in the atmosphere? *Geophysical Research Letters*, *38*, L08803. http://dx.doi.org/10.1029/2011GL046654.

Babu, S. S., Moorthy, K. K., & Satheesh, S. K. (2007). Temporal heterogeneity in aerosol characteristics and the resulting radiative impacts at a tropical coastal station – Part 2: Direct short wave radiative forcing. *Annales Geophysicae*, *25*, 2309–2320.

Babu, S. S., Nair, V. S., Gogoi, M. M., & Moorthy, K. K. (2015). Seasonal variation of vertical distribution of aerosol single scattering albedo over Indian sub-continent: RAWEX aircraft observations. *Atmospheric Environment*, 1–12.

Banerjee, T., Kumar, M., Mall, R. K., & Singh, R. S. (2017b). Airing 'clean air' in clean India mission. *Environmental Science and Pollution Research*, *24*, 6399–6413.

Banerjee, T., Murari, V., Kumar, M., & Raju, M. P. (2015). Source apportionment of airborne particulates through receptor modeling: Indian scenario. *Atmospheric Research*, *164*(*165*), 167–187.

Bisht, D. S., Dumka, U. C., Kaskaoutis, D. G., Pipal, A. S., Srivastava, A. K., Soni, V. K., et al. (2015). Carbonaceous aerosols and pollutants over Delhi urban environment: Temporal evolution, source apportionment and radiative forcing. *Science of the Total Environment*, *521–522*, 431–445.

Bollasina, M., Nigam, S., & Lau, K. M. (2008). Absorbing aerosols and summer monsoon evolution over South Asia: An observational portrayal. *Journal of Climate*, *21*, 3221–3239.
Bond, T. C., Doherty, S. J., Fahey, D. W., Forster, P. M., Berntsen, T., De Angelo, B. J., et al. (2013). Bounding the role of black carbon in the climate system: A scientific assessment. *Journal of Geophysical Research*, *118*, 5380–5552.
Bond, T. C., Streets, D. G., Yarber, K. F., Nelson, S. M., Woo, J. H., & Klimont, Z. (2004). A technology-based global inventory of black and organic carbon emissions from combustion. *Journal of Geophysical Research*, *109*, D14203.
Das, S. K., & Jayaraman, A. (2011). Role of black carbon in aerosol properties and radiative forcing over western India during premonsoon period. *Atmospheric Research*, *102*, 320–334.
Draxler, R. R., & Rolph, G. D. (2003). *HYSPLIT (HYbridSingle-Particle Lagrangian IntegratedTrajectory) Model Access Via NOAA ARL READY Website*. Silver Spring, MD: NOAA Air ResourcesLaboratory. http://www.arl.noaa.gov/ready/hysplit4.html.
Fochesatto, G. J., Drobinski, F., Flamant, C., Guedalia, D., Sarrat, C., Flamant, P. H., et al. (2001). Evidence of dynamical coupling between the residual layer and the developing convective boundary layer. *Boundary Layered Meteorology*, *99*(*3*), 451–464.
Hansen, A. D. A., Rosen, H., & Novakov, T. (1984). The aethalometer—an instrument for the real-time measurement of optical absorption by aerosol particles. *Science of the Total Environment*, *36*, 191–196.
Hess, M., Koepke, P., & Schult, I. (1998). Optical properties of aerosols and clouds: The software package OPAC. *Bulletin of the American Meteorological Society*, *79*(*5*), 831–844.
http://www.imd.gov.in/pages/monsoon_main.php. Monsoon. India Meteorological Department, Ministry of Earth Science, Govt. of India. Accessed on January 2016).
IPCC (2007). *Intergovernmental panel on climate change. Climate change: The physical science basis*. New York: Cambridge University Press, 131–216.
IPCC (2014). *Intergovernmental panel on climate change. Climate change: The physical science basis*. New York: Cambridge University Press, 659–720.
Jin, Q., Wei, J., & Yang, Z. L. (2014). Positive response of Indian summer rainfall to Middle East dust. *Geophysical Research Letters*, *41*, 4068–4074. http://dx.doi.org/10.1002/2014gl059980.
Jin, Q., Wei, J., Yang, Z. L., Pu, B., & Huang, J. (2015). Consistent response of Indian summer monsoon to Middle East dust in observations and simulations. *Atmospheric Chemistry and Physics Discussions*, *15*, 15571–15619. http://dx.doi.org/10.5194/acpd-15-15571-2015.
Jin, Q., Yang, Z. L., & Wei, J. (2016). High sensitivity of Indian summer monsoon to Middle East dust absorptive properties. *Scientific Reports*, *6*. http://dx.doi.org/10.1038/srep30690.
Koren, I., Kaufman, Y. J., Remer, L. A., & Martins, J. V. (2004). Measurement of the effect of Amazon smoke on inhibition of cloud formation. *Science*, *303*, 1342–1345.
Kumar, M., Raju, M. P., Singh, R. K., Singh, A. K., Singh, R. S., & Banerjee, T. (2017). Wintertime characteristics of aerosols over middle Indo-Gangetic Plain: Vertical profile, transport and radiative forcing. *Atmospheric Research*, *183*, 268–282.
Kumar, M., Singh, R. K., Murari, V., Singh, A. K., Singh, R. S., & Banerjee, T. (2016). Fireworks induced particle pollution: A spatio-temporal analysis. *Atmospheric Research*, *180*, 78–91.
Kumar, M., Tiwari, S., Murari, V., Singh, A. K., & Banerjee, T. (2015). Wintertime characteristics of aerosols at middle Indo-Gangetic Plain: Impacts of regional meteorology and long range transport. *Atmospheric Environm*, *104*, 162–175.
Lamarque, J. F., Bond, T. C., Eyring, V., Granier, C., Heil, A., Klimont, Z., et al. (2010). Historical (1850–2000) gridded anthropogenic and biomass burning emissions of reactive gases and aerosols: Methodology and application. *Atmospheric Chemistry*, *10*, 7017–7039.
Lau, K. M., & Kim, K. M. (2006). Observational relationships between aerosol and Asian monsoon rainfall, and circulation. *Geophysical Research Letters*, *33*, L21810.
Lau, K. M., Kim, M. K., & Kim, K. M. (2006). Asian summer monsoon anomalies induced by aerosol direct forcing: The role of the Tibetan Plateau. *Climate Dynamic*, *26*, 855–864.
Lee, W.-S., & Kim, M.-K. (2010). Effects of radiative forcing by black carbon aerosol on spring rainfall decrease over Southeast Asia. *Atmospheric Environment*, *44*(*2010*), 3739–3744.
Manoj, M. G., Devara, P. C. S., Safai, P. D., & Goswami, B. N. (2010). Absorbing aerosols facilitate transition of Indian monsoon breaks to active spells. *Climate Dynamic*, *37*, 2181–2198.
Meehl, G. A., Arblaster, J. M., & Collins, W. D. (2008). Effects of black carbon aerosols on the Indian monsoon. *Journal Climate*, *21*, 2869–2882.
Menon, H. B., Shirodkar, S., Kedia, S., Ramachandran, S., Babu, S. S., & Moorthy, K. K. (2014). Temporal variation of aerosol optical depth and associated shortwave radiative forcing over a coastal site along the west coast of India. *Science of the Total Environment*, *468–469*, 83–92.
Murari, V., Kumar, M., Mhawish, A., Barman, S. C., & Banerjee, T. (2017). Airborne particulate in Varanasi over middle Indo-Gangetic Plain: Variation in particulate types and meteorological influences. *Environmental Monitoring and Assessment*. http://dx.doi.org/10.1007/s10661-017-5859-9.
Murari, V., Kumar, M., Singh, N., Singh, R. S., & Banerjee, T. (2016). Particulate morphology and elemental characteristics: Variability at middle Indo-Gangetic Plain. *Journal of Atmospheric Chemistry*, *73*, 165–179.
Myhre, G., Shindell, D., Bréon, F.-M., Collins, W., Fuglestvedt, J., Huang, J., ... Zhang, H. (2013). Anthropogenic and natural radiative forcing. In T. F. Stocker,, D. Qin,, G.-K. Plattner,, M. Tignor,, S. K. Allen,, & J. Boschung, (Eds.), *Climate change 2013: The physical science basis. Contribution of working group I to the fifth assessment report of the intergovernmental panel on climate change*. Cambridge, United Kingdom and New York, NY, USA: Cambridge University Press.
Pathak, B., Kalita, G., Bhuyan, K., Bhuyan, P. K., & Moorthy, K. K. (2010). Aerosol temporal characteristics and its impact on shortwave radiative forcing at a location in the northeast of India. *Journal of Geophysical Research*, *115*, D19204.
Raju, M. P., Safai, P. D., Sonbawne, S. M., & Naidu, C. V. (2015). Black carbon radiative forcing over the Indian Arctic station, Himadri during the Arctic Summer of 2012. *Atmospheric Research*, *157*, 29–36.
Raju, M. P., Safai, P. D., Vijayakumar, K., Devara, P. C. S., Naidu, C. V., Rao, P. S. P., & Pandithurai, G. (2016). Atmospheric abundances of black carbon aerosols and their radiative impact over an urban and a rural site in SW India. *Atmospheric Environment*, *125*, 429–436.
Ramachandran, S., & Kedia, S. (2010). Black carbon aerosols over an urban region: Radiative forcing and climate impact. *Journal of Geophysical Research*, *115*, D10202.
Ramanathan, V., Chung, C., Kim, D., Bettge, T., Buja, L., Kiehl, J. T., et al. (2005). Atmospheric brown clouds: Impacts on south Asian climate and hydrological cycle. *Proceedings of the National Academy of Sciences of the USA*, *102*(*15*), 5326–5333.
Ramanathan, V., Crutzen, P. J., Kiehl, J. T., & Rosenfeld, D. (2001). Aerosols, climate, and the hydrological cycle. *Science*, *294*, 2119–2124.
Remer, L. A., Kaufman, Y. J., Tanre, D., Matto, S., Chu, D. A., Martins, J. V., et al. (2005). The MODIS aerosol algorithm, products, and validation. *Journal of the Atmospheric Sciences*, *62*, 947–973.
Ricchiazzi, P., Yang, S., Gautier, C., & Sowle, D. (1998). SBDART: A research and teaching software tool for plane-parallel radiative transfer in the Earth's atmosphere. *Bulletin of the American Meteorological Society*, *79*, 2101–2114.
Rosenfeld, D., Rudich, Y., & Lahav, R. (2001). Desert dust suppressing precipitation: A possible desertification feedback loop. *Proceedings of the National Academy of Sciences USA*, *98*, 5975–5980.
Safai, P. D., Raju, M. P., Budhavant, K. B., Rao, P. S. P., & Devara, P. C. S. (2013). Long term studies on characteristics of black carbon aerosols over a tropical urban station Pune, India. *Atmospheric Research*, *132–133*, 173–184.
Sanap, S. D., & Pandithurai, G. (2015). The effect of absorbing aerosols on Indian monsoon circulation and rainfall: A review. *Atmospheric Research*, *164–165*, 318–327.
Sarkar, C., Chatterjee, A., Singh, A. K., Ghosh, S. K., & Raha, S. (2015). Characterization of black carbon aerosols over Darjeeling - a high altitude Himalayan station in Eastern India. *Aerosol and Air Quality Research*, *15*, 465–478.
Sen, A., Abdelmaksoud, A. S., Nazeer Ahammed, Y., Alghamdi, M. E., Banerjee, T., et al. (2017). Variations in particulate matter over Indo-Gangetic Plains and Indo-Himalayan Range during four field campaigns in winter monsoon and summer monsoon: Role of pollution pathways. *Atmospheric Environment*. http://dx.doi.org/10.1016/j.atmosenv.2016.12.054.
Sen, A., Ahammed, Y. N., Banerjee, T., Chatterjee, A., Choudhuri, A. K., Das, T., et al. (2016). Spatial variability in ambient atmospheric fine and coarse mode aerosols over Indo-Gangetic plains, India and adjoining oceans during the onset of summer monsoons, 2014. *Atmospheric Pollution Research*, *7*, 521–532.
Shukla, K., Srivastava, P. K., Banerjee, T., & Aneja, V. P. (2017). Trend and variability of atmospheric ozone over middle Indo-Gangetic Plain: Impacts of seasonality and precursor gases. *Environmental Science and Pollution Research*, *24*, 164–179.
Singh, N., Mhawish, A., Deboudt, K., Singh, R. S., & Banerjee, T. (2017b). Organic aerosols over Indo-Gangetic Plain: Sources, distributions and climatic implications.

Atmospheric Environment, *157*, 59–74.
Singh, N., Murari, V., Kumar, M., Barman, S. C., & Banerjee, T. (2017a). Fine particulates over South Asia: Review and meta-analysis of PM2.5 source apportionment through receptor model. *Environmental Pollution*, *223*, 121–136.
Sreekanth, V., Niranjan, K., & Madhavan, B. L. (2007). Radiative forcing of black carbon over eastern India. *Geophysical Research Letters*, *34*, L17818. http://dx.doi.org/10.1029/2007GL030377.
Surendran, D. E., Beig, G., Ghude, S. D., Panicker, A. S., Manoj, M. G., Chate, D. E., et al. (2013). Radiative forcing of black carbon over Delhi. *International Journal of Photoenergy*, *313652*, 7.
Tyagi, A., Hatwar, H. R., & Pai, D. S. (2010). *Monsoon 2009: A report. IMD: Synoptic meteorology 2010; No: 09/2010*⟨http://www.imd.gov.in/section/nhac/dynamic/monsoon_report_2009.pdf⟩.
Venkataraman, C., Habib Fernandez, A. E., Miguel, A. H., & Friedlander, S. K. (2005). Residential biofuels in south Asia: Carbonaceous aerosol emissions and climate impacts. *Science*, *307*(*5714*), 1454–1456.
Virkkula, A., Makela, T., Hillamo, R., Yli-Tuomi, T., Hirsikko, A., Hameri, K., et al. (2007). A simple procedure for correcting loading effects of Aethalometer. *Journal of the Air and Waste Management Associations*, *57*, 1214–1222.
Wang, C. (2004). A modeling study on the climate impacts of black carbon aerosols. *Journal of Geophysical Research*, *109*, D03106. http://dx.doi.org/10.1029/2003JD004084.
Wang, C. (2007). Impact of direct radiative forcing of black carbon aerosols on tropical convective precipitation. *Geophysics Research Letter*, *34*, 1–6.